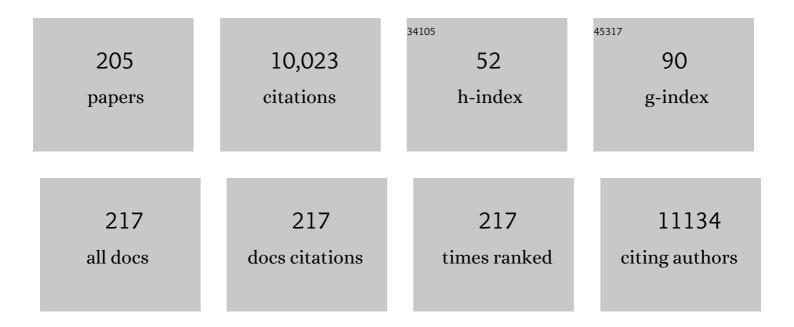
## Jeong Woo Han

List of Publications by Year in descending order

Source: https://exaly.com/author-pdf/323667/publications.pdf Version: 2024-02-01



#	Article	IF	CITATIONS
1	Dynamic Surface Evolution of Metal Oxides for Autonomous Adaptation to Catalytic Reaction Environments. Advanced Materials, 2023, 35, .	21.0	1
2	Alleviating inhibitory effect of H2 on low-temperature water-gas shift reaction activity of Pt/CeO2 catalyst by forming CeO2 nano-patches on Pt nano-particles. Applied Catalysis B: Environmental, 2022, 305, 121038.	20.2	11
3	Precisely Constructing Orbital Coupling-Modulated Dual-Atom Fe Pair Sites for Synergistic CO <sub>2</sub> Electroreduction. ACS Energy Letters, 2022, 7, 640-649.	17.4	127
4	Continuous Oxygen Vacancy Gradient in TiO <sub>2</sub> Photoelectrodes by a Photoelectrochemicalâ€Driven "Selfâ€Purification―Process. Advanced Energy Materials, 2022, 12, .	19.5	42
5	Universally characterizing atomistic strain via simulation, statistics, and machine learning: Low-angle grain boundaries. Acta Materialia, 2022, 226, 117635.	7.9	5
6	Structural changes of hydrotalcite-based Co-containing mixed oxides with calcination temperature and their effects on NOx adsorption: A combined experimental and DFT study. Chemical Engineering Journal, 2022, 437, 135209.	12.7	6
7	Utilization of an Isovalent Doping Strategy in Cobalt-Free Ferrites for Highly Active and Stable Solid Oxide Fuel Cell Cathodes. ACS Applied Energy Materials, 2022, 5, 3417-3425.	5.1	6
8	Boosting Support Reducibility and Metal Dispersion by Exposed Surface Atom Control for Highly Active Supported Metal Catalysts. ACS Catalysis, 2022, 12, 4402-4414.	11.2	19
9	Computational Screening of Single-Metal-Atom Embedded Graphene-Based Electrocatalysts Stabilized by Heteroatoms. Frontiers in Chemistry, 2022, 10, 873609.	3.6	6
10	Metal–nitrogen–carbon-based nanozymes: advances and perspectives. Journal Physics D: Applied Physics, 2022, 55, 323001.	2.8	6
11	High-performance hysteresis-free perovskite transistors through anion engineering. Nature Communications, 2022, 13, 1741.	12.8	51
12	Surface Roughening Strategy for Highly Efficient Bifunctional Electrocatalyst: Combination of Atomic Layer Deposition and Anion Exchange Reaction. Small Methods, 2022, 6, e2101308.	8.6	15
13	Rational Development of Coâ€Doped Mesoporous Ceria with High Peroxidaseâ€Mimicking Activity at Neutral pH for Paperâ€Based Colorimetric Detection of Multiple Biomarkers. Advanced Functional Materials, 2022, 32, .	14.9	39
14	Precise control of surface oxygen vacancies in ZnO nanoparticles for extremely high acetone sensing response. Journal of Advanced Ceramics, 2022, 11, 769-783.	17.4	33
15	Crystal Facet-Manipulated 2D Pt Nanodendrites to Achieve an Intimate Heterointerface for Hydrogen Evolution Reactions. Journal of the American Chemical Society, 2022, 144, 9033-9043.	13.7	53
16	Titanium Monoxide with <i>in Situ</i> Grown Rutile TiO <sub>2</sub> Nanothorns as a Heterostructured Job-Sharing Anode Material for Lithium-Ion Storage. ACS Applied Energy Materials, 2022, 5, 5691-5703.	5.1	5
17	Concurrent promotion of phase transition and bimetallic nanocatalyst exsolution in perovskite oxides driven by Pd doping to achieve highly active bifunctional fuel electrodes for reversible solid oxide electrochemical cells. Applied Catalysis B: Environmental, 2022, 314, 121517.	20.2	16
18	Precise Modulation of Tripleâ€Phase Boundaries towards a Highly Functional Exsolved Catalyst for Dry Reforming of Methane under a Dilutionâ€Free System. Angewandte Chemie, 2022, 134, .	2.0	2

#	Article	IF	CITATIONS
19	Precise Modulation of Tripleâ€Phase Boundaries towards a Highly Functional Exsolved Catalyst for Dry Reforming of Methane under a Dilutionâ€Free System. Angewandte Chemie - International Edition, 2022, 61, .	13.8	12
20	Manipulating the Resistive Switching in Epitaxial SrCoO <sub>2.5</sub> Thin-Film-Based Memristors by Strain Engineering. ACS Applied Electronic Materials, 2022, 4, 2729-2738.	4.3	5
21	Role of an Interface for Hydrogen Production Reaction over Size-Controlled Supported Metal Catalysts. ACS Catalysis, 2022, 12, 8082-8093.	11.2	9
22	Tuning electrochemical water oxidation towards ozone evolution with heterojunction anode architectures. Journal of Materials Chemistry A, 2022, 10, 17132-17141.	10.3	3
23	Promoting biomass electrooxidation via modulating proton and oxygen anion deintercalation in hydroxide. Nature Communications, 2022, 13, .	12.8	60
24	Adenine oligomer directed synthesis of chiral gold nanoparticles. Nature Communications, 2022, 13, .	12.8	31
25	Design of grain boundary enriched bimetallic borides for enhanced hydrogen evolution reaction. Chemical Engineering Journal, 2021, 405, 126977.	12.7	56
26	Key Roles of Trace Oxygen Treatment for Highâ€Performance Znâ€Đoped Cul pâ€Channel Transistors. Advanced Electronic Materials, 2021, 7, .	5.1	17
27	Corrosion-engineered bimetallic oxide electrode as anode for high-efficiency anion exchange membrane water electrolyzer. Chemical Engineering Journal, 2021, 420, 127670.	12.7	51
28	Interface-modulated uniform outer nanolayer: A category of electrodes of nanolayer-encapsulated core-shell configuration for supercapacitors. Nano Energy, 2021, 81, 105667.	16.0	48
29	Unprecedented electrocatalytic oxygen evolution performances by cobalt-incorporated molybdenum carbide microflowers with controlled charge re-distribution. Journal of Materials Chemistry A, 2021, 9, 1770-1783.	10.3	13
30	Mechanistic insights into the phase transition and metal ex-solution phenomena of Pr <sub>0.5</sub> Ba <sub>0.5</sub> Mn <sub>0.85</sub> Co <sub>0.15</sub> O <sub>3â^'δ</sub> from simple to layered perovskite under reducing conditions and enhanced catalytic activity. Energy and Environmental Science, 2021, 14, 873-882.	30.8	37
31	Reconstructing the Coordination Environment of Platinum Single-Atom Active Sites for Boosting Oxygen Reduction Reaction. ACS Catalysis, 2021, 11, 466-475.	11.2	62
32	Tailoring Binding Abilities by Incorporating Oxophilic Transition Metals on 3D Nanostructured Ni Arrays for Accelerated Alkaline Hydrogen Evolution Reaction. Journal of the American Chemical Society, 2021, 143, 1399-1408.	13.7	161
33	Ultrathin and Bifunctional Polymer-Nanolayer-Embedded Separator to Simultaneously Alleviate Li Dendrite Growth and Polysulfide Crossover in Li–S Batteries. ACS Applied Energy Materials, 2021, 4, 611-622.	5.1	20
34	Atomic layer deposition-triggered hierarchical core/shell stable bifunctional electrocatalysts for overall water splitting. Journal of Materials Chemistry A, 2021, 9, 21132-21141.	10.3	10
35	2D-structured V-doped Ni(Co,Fe) phosphides with enhanced charge transfer and reactive sites for highly efficient overall water splitting electrocatalysts. Journal of Materials Chemistry A, 2021, 9, 12203-12213.	10.3	45
36	Engineering electrocatalyst nanosurfaces to enrich the activity by inducing lattice strain. Energy and Environmental Science, 2021, 14, 3717-3756.	30.8	98

#	Article	IF	CITATIONS
37	Progress of Exsolved Metal Nanoparticles on Oxides as High Performance (Electro)Catalysts for the Conversion of Small Molecules. Small, 2021, 17, e2005383.	10.0	53
38	Simple physical mixing of zeolite prevents sulfur deactivation of vanadia catalysts for NOx removal. Nature Communications, 2021, 12, 901.	12.8	49
39	Effect of Monovalent Metal Iodide Additives on the Optoelectric Properties of Two-Dimensional Sn-Based Perovskite Films. Chemistry of Materials, 2021, 33, 2498-2505.	6.7	28
40	One-Pot Chemo-bioprocess of PET Depolymerization and Recycling Enabled by a Biocompatible Catalyst, Betaine. ACS Catalysis, 2021, 11, 3996-4008.	11.2	58
41	Molecular alignment descriptor to search for the most stable adsorption sites of saturated cyclic compounds on metal surfaces. Applied Surface Science, 2021, 544, 148904.	6.1	4
42	Intermediates for catalytic reduction of CO2 on p-block element surfaces. Journal of Industrial and Engineering Chemistry, 2021, 96, 236-242.	5.8	20
43	The association between L1 skeletal muscle index derived from routine CT and in-hospital mortality in CAP patients in the ED. American Journal of Emergency Medicine, 2021, 42, 49-54.	1.6	6
44	Disordered-Layer-Mediated Reverse Metal–Oxide Interactions for Enhanced Photocatalytic Water Splitting. Nano Letters, 2021, 21, 5247-5253.	9.1	18
45	Universal prediction of strain footprints via simulation, statistics, and machine learning: low-Σ grain boundaries. Acta Materialia, 2021, 211, 116850.	7.9	5
46	Enhancing Thermocatalytic Activities by Upshifting the dâ€Band Center of Exsolved Coâ€Niâ€Fe Ternary Alloy Nanoparticles for the Dry Reforming of Methane. Angewandte Chemie, 2021, 133, 16048-16055.	2.0	11
47	Probing an Interfacial Ionic Pairingâ€Induced Molecular Dipole Effect in Ionovoltaic System. Small Methods, 2021, 5, e2100323.	8.6	6
48	Improved Catalytic Activity of the High-Temperature Water Gas Shift Reaction on Metal-Exsolved La0.9Ni0.05Fe0.95O3 by Controlling Reduction Time. ChemEngineering, 2021, 5, 28.	2.4	3
49	Highâ€Efficiency Anionâ€Exchange Membrane Water Electrolyzer Enabled by Ternary Layered Double Hydroxide Anode. Small, 2021, 17, e2100639.	10.0	49
50	Structure-activity relationship of VO /TiO2 catalysts for mercury oxidation: A DFT study. Applied Surface Science, 2021, 552, 149462.	6.1	17
51	Enhancing Thermocatalytic Activities by Upshifting the dâ€Band Center of Exsolved Coâ€Niâ€Fe Ternary Alloy Nanoparticles for the Dry Reforming of Methane. Angewandte Chemie - International Edition, 2021, 60, 15912-15919.	13.8	65
52	Anion Exchange Membrane Water Electrolysis: Highâ€Efficiency Anionâ€Exchange Membrane Water Electrolyzer Enabled by Ternary Layered Double Hydroxide Anode (Small 28/2021). Small, 2021, 17, 2170147.	10.0	1
53	Facet-Dependent Mn Doping on Shaped Co <sub>3</sub> O <sub>4</sub> Crystals for Catalytic Oxidation. ACS Catalysis, 2021, 11, 11066-11074.	11.2	69
54	Engineering Single Atom Catalysts to Tune Properties for Electrochemical Reduction and Evolution Reactions. Advanced Energy Materials, 2021, 11, 2101670.	19.5	42

#	Article	IF	CITATIONS
55	Exsolved metal-boosted active perovskite oxide catalyst for stable water gas shift reaction. Journal of Catalysis, 2021, 400, 148-159.	6.2	18
56	A stable and active three-dimensional carbon based trimetallic electrocatalyst for efficient overall wastewater splitting. International Journal of Hydrogen Energy, 2021, 46, 30762-30779.	7.1	9
57	Tuning reaction pathways of peroxymonosulfate-based advanced oxidation process via defect engineering. Cell Reports Physical Science, 2021, 2, 100550.	5.6	9
58	Polymer Interface-Dependent Morphological Transition toward Two-Dimensional Porous Inorganic Nanocoins as an Ultrathin Multifunctional Layer for Stable Lithium–Sulfur Batteries. Journal of the American Chemical Society, 2021, 143, 15644-15652.	13.7	22
59	Chemical transformation approach for high-performance ternary NiFeCo metal compound-based water splitting electrodes. Applied Catalysis B: Environmental, 2021, 294, 120246.	20.2	67
60	Synergistic coupling ensuing cobalt phosphosulfide encapsulated by heteroatom-doped two-dimensional graphene shell as an excellent catalyst for oxygen electroreduction. Chemical Engineering Journal, 2021, 423, 130233.	12.7	10
61	In-situ exsolution of Ni nanoparticles to achieve an active and stable solid oxide fuel cell anode catalyst on A-site deficient La0.4Sr0.4Ti0.94Ni0.06O3-δ. Journal of Industrial and Engineering Chemistry, 2021, 103, 264-274.	5.8	17
62	Various metal (Fe, Mo, V, Co)-doped Ni2P nanowire arrays as overall water splitting electrocatalysts and their applications in unassisted solar hydrogen production with STH 14 %. Applied Catalysis B: Environmental, 2021, 297, 120434.	20.2	82
63	Multidentate thia-crown ethers as hyper-crosslinked macroporous adsorbent resins for the efficient Pd/Pt recovery and separation from highly acidic spent automotive catalyst leachate. Chemical Engineering Journal, 2021, 424, 130379.	12.7	21
64	Continuous Synthesis of Methanol from Methane and Steam over Copper-Mordenite. ACS Catalysis, 2021, 11, 1065-1070.	11.2	28
65	Design principles of noble metal-free electrocatalysts for hydrogen production in alkaline media: combining theory and experiment. Nanoscale Advances, 2021, 3, 6797-6826.	4.6	23
66	Effective Screening Route for Highly Active and Selective Metalâ^'Nitrogenâ€Doped Carbon Catalysts in CO <sub>2</sub> Electrochemical Reduction. Small, 2021, 17, e2103705.	10.0	12
67	Activating Lattice Oxygen in Perovskite Oxide by Bâ€Site Cation Doping for Modulated Stability and Activity at Elevated Temperatures. Advanced Science, 2021, 8, e2102713.	11.2	44
68	Engineering counter-ion-induced disorder of a highly doped conjugated polymer for high thermoelectric performance. Nano Energy, 2021, 90, 106604.	16.0	17
69	Unveiling the key factor for the phase reconstruction and exsolved metallic particle distribution in perovskites. Nature Communications, 2021, 12, 6814.	12.8	28
70	Systematic Approach to Designing a Highly Efficient Core–Shell Electrocatalyst for N <sub>2</sub> O Reduction. ACS Catalysis, 2021, 11, 15089-15097.	11.2	9
71	Density functional theory study on the dehydrogenation of 1,2-dimethyl cyclohexane and 2-methyl piperidine on Pd and Pt catalysts. Catalysis Today, 2020, 352, 345-353.	4.4	30
72	Design of Ceria Catalysts for Lowâ€īemperature CO Oxidation. ChemCatChem, 2020, 12, 11-26.	3.7	78

#	Article	IF	CITATIONS
73	Heme Cofactorâ€Resembling Fe–N Single Site Embedded Graphene as Nanozymes to Selectively Detect H <sub>2</sub> O <sub>2</sub> with High Sensitivity. Advanced Functional Materials, 2020, 30, 1905410.	14.9	171
74	The position of lysine controls the catechol-mediated surface adhesion and cohesion in underwater mussel adhesion. Journal of Colloid and Interface Science, 2020, 563, 168-176.	9.4	51
75	Size-Controlled Pd Nanoparticles Loaded on Co <sub>3</sub> O <sub>4</sub> Nanoparticles by Calcination for Enhanced CO Oxidation. ACS Applied Nano Materials, 2020, 3, 486-495.	5.0	26
76	Room-Temperature-Processed Amorphous Sn-In-O Electron Transport Layer for Perovskite Solar Cells. Materials, 2020, 13, 32.	2.9	7
77	Oxidative Methane Conversion to Ethane on Highly Oxidized Pd/CeO <sub>2</sub> Catalysts Below 400 °C. ChemSusChem, 2020, 13, 677-681.	6.8	16
78	Dopantâ€Driven Positive Reinforcement in Exâ€Solution Process: New Strategy to Develop Highly Capable and Durable Catalytic Materials. Advanced Materials, 2020, 32, e2003983.	21.0	26
79	Quantum Dots of [Na <sub>4</sub> Cs <sub>6</sub> PbBr <sub>4</sub> ] <sup>8+</sup> , Water Stable in Zeolite X, Luminesce Sharply in the Green. Advanced Materials, 2020, 32, e2001868.	21.0	14
80	Catalytic Materials: Dopantâ€Driven Positive Reinforcement in Exâ€Solution Process: New Strategy to Develop Highly Capable and Durable Catalytic Materials (Adv. Mater. 46/2020). Advanced Materials, 2020, 32, 2070342.	21.0	1
81	Effects of Hydrogen on the Stacking Orientation of Bilayer Graphene Grown on Copper. Chemistry of Materials, 2020, 32, 10357-10364.	6.7	10
82	Computational approaches to the exsolution phenomenon in perovskite oxides with a view to design highly durable and active anodes for solid oxide fuel cells. Korean Journal of Chemical Engineering, 2020, 37, 1295-1305.	2.7	9
83	Controlling the Oxidation State of Pt Single Atoms for Maximizing Catalytic Activity. Angewandte Chemie, 2020, 132, 20872-20877.	2.0	28
84	Controlling the Oxidation State of Pt Single Atoms for Maximizing Catalytic Activity. Angewandte Chemie - International Edition, 2020, 59, 20691-20696.	13.8	113
85	Validation of defect association energy on modulating oxygen ionic conductivity in low temperature solid oxide fuel cell. Journal of Power Sources, 2020, 480, 229106.	7.8	10
86	Probing One-Dimensional Oxygen Vacancy Channels Driven by Cation–Anion Double Ordering in Perovskites. Nano Letters, 2020, 20, 8353-8359.	9.1	12
87	Structural Design of Amorphous CoMoP <i><sub>x</sub></i> with Abundant Active Sites and Synergistic Catalysis Effect for Effective Water Splitting. Advanced Functional Materials, 2020, 30, 2003889.	14.9	128
88	Highly active dry methane reforming catalysts with boosted in situ grown Ni-Fe nanoparticles on perovskite via atomic layer deposition. Science Advances, 2020, 6, eabb1573.	10.3	79
89	Design of an Ultrastable and Highly Active Ceria Catalyst for CO Oxidation by Rare-Earth- and Transition-Metal Co-Doping. ACS Catalysis, 2020, 10, 14877-14886.	11.2	23
90	Control of transition metal–oxygen bond strength boosts the redox ex-solution in a perovskite oxide surface. Energy and Environmental Science, 2020, 13, 3404-3411.	30.8	36

#	Article	IF	CITATIONS
91	Nb-TiO2 nanotubes as catalyst supports with high activity and durability for oxygen reduction. Applied Surface Science, 2020, 521, 146330.	6.1	14
92	Development of Ni-based alloy catalysts to improve the sulfur poisoning resistance of Ni/YSZ anodes in SOFCs. Catalysis Science and Technology, 2020, 10, 4544-4552.	4.1	10
93	Identifying the electrocatalytic active sites of a Ru-based catalyst with high Faraday efficiency in CO <sub>2</sub> -saturated media for an aqueous Zn–CO <sub>2</sub> system. Journal of Materials Chemistry A, 2020, 8, 14927-14934.	10.3	16
94	Directional Change of Interfacial Electric Field by Carbon Insertion in Heterojunction System TiO <sub>2</sub> /WO <sub>3</sub> . ACS Applied Materials & Interfaces, 2020, 12, 15239-15245.	8.0	32
95	Plasmaâ€Assisted Catalytic Effects of TiO <sub>2</sub> /Macroporous SiO <sub>2</sub> on the Synthesis of Light Hydrocarbons from Methane. ChemCatChem, 2020, 12, 5067-5075.	3.7	5
96	Highly selective extraction of palladium from spent automotive catalyst acid leachate using novel alkylated dioxa-dithiacrown ether derivatives. Journal of Industrial and Engineering Chemistry, 2020, 89, 428-435.	5.8	18
97	Highâ€Performance and Reliable Leadâ€Free Layeredâ€Perovskite Transistors. Advanced Materials, 2020, 32, e2002717.	21.0	86
98	Simultaneous Suppression of Shuttle Effect and Lithium Dendrite Growth by Lightweight Bifunctional Separator for Li–S Batteries. ACS Applied Energy Materials, 2020, 3, 2643-2652.	5.1	34
99	Catalytic decomposition of N2O on Pd Cu alloy catalysts: A density functional theory study. Applied Surface Science, 2020, 510, 145349.	6.1	20
100	Pd–Cu alloy catalyst synthesized by citric acid-assisted galvanic displacement reaction for N2O reduction. Journal of Applied Electrochemistry, 2020, 50, 395-405.	2.9	6
101	Engineering of Charged Defects at Perovskite Oxide Surfaces for Exceptionally Stable Solid Oxide Fuel Cell Electrodes. ACS Applied Materials & Interfaces, 2020, 12, 21494-21504.	8.0	43
102	A review of smart exsolution catalysts for the application of gas phase reactions. Ceramist, 2020, 23, 211-230.	0.1	2
103	Enantiospecific Adsorption and Decomposition of Cysteine Enantiomers on the Chiral Cu{421} <sup>R</sup> Surface. Journal of Physical Chemistry C, 2019, 123, 20829-20837.	3.1	8
104	Density functional theory study of NOx adsorption on alkaline earth metal oxide and transition metal surfaces. Korean Journal of Chemical Engineering, 2019, 36, 1258-1266.	2.7	7
105	Investigation of the Support Effect in Atomically Dispersed Pt on WO 3â^' x for Utilization of Pt in the Hydrogen Evolution Reaction. Angewandte Chemie, 2019, 131, 16184-16188.	2.0	49
106	Investigation of the Support Effect in Atomically Dispersed Pt on WO <sub>3â^'<i>x</i></sub> for Utilization of Pt in the Hydrogen Evolution Reaction. Angewandte Chemie - International Edition, 2019, 58, 16038-16042.	13.8	271
107	Controlling Electrostatic Interaction in PEDOT:PSS to Overcome Thermoelectric Tradeoff Relation. Advanced Functional Materials, 2019, 29, 1905590.	14.9	60
108	Transparent Conductive Films Derived from Single-Walled Aluminosilicate Nanotubes. ACS Applied Nano Materials, 2019, 2, 6677-6689.	5.0	5

#	Article	IF	CITATIONS
109	Improved CO Oxidation via Surface Stabilization of Ceria Nanoparticles Induced by Rare-Earth Metal Dopants. ACS Applied Nano Materials, 2019, 2, 6473-6481.	5.0	13
110	Highly Water-Resistant La-Doped Co <sub>3</sub> O <sub>4</sub> Catalyst for CO Oxidation. ACS Catalysis, 2019, 9, 10093-10100.	11.2	126
111	Aqueous Synthesis of 14â€15â€Membered Crown Ethers with Mixed O, N and S Heteroatoms: Experimental and Theoretical Binding Studies with Platinumâ€Group Metals. ChemPlusChem, 2019, 84, 210-221.	2.8	11
112	A new etching process for zinc oxide with etching rate and crystal plane control: experiment, calculation, and membrane application. Nanoscale, 2019, 11, 12337-12346.	5.6	3
113	Rational Design of Transition Metal Coâ€doped Ceria Catalysts for Lowâ€Temperature CO Oxidation. ChemCatChem, 2019, 11, 2225-2225.	3.7	0
114	Rational Design of Transition Metal Coâ€Doped Ceria Catalysts for Lowâ€Temperature CO Oxidation. ChemCatChem, 2019, 11, 2288-2296.	3.7	26
115	Versatile Strategy for Tuning ORR Activity of a Single Fe-N <sub>4</sub> Site by Controlling Electron-Withdrawing/Donating Properties of a Carbon Plane. Journal of the American Chemical Society, 2019, 141, 6254-6262.	13.7	509
116	Growth Kinetics of Individual Co Particles Ex-solved on SrTi <sub>0.75</sub> Co <sub>0.25</sub> O <sub>3-î´</sub> Polycrystalline Perovskite Thin Films. Journal of the American Chemical Society, 2019, 141, 6690-6697.	13.7	75
117	Cation-swapped homogeneous nanoparticles in perovskite oxides for highÂpower density. Nature Communications, 2019, 10, 697.	12.8	119
118	Modified carbon nitride nanozyme as bifunctional glucose oxidase-peroxidase for metal-free bioinspired cascade photocatalysis. Nature Communications, 2019, 10, 940.	12.8	349
119	A Highly Active and Redox-Stable SrGdNi <sub>0.2</sub> Mn <sub>0.8</sub> O <sub>4±Î′</sub> Anode with in Situ Exsolution of Nanocatalysts. ACS Catalysis, 2019, 9, 1172-1182.	11.2	62
120	Approaching Ultrastable Highâ€Rate Li–S Batteries through Hierarchically Porous Titanium Nitride Synthesized by Multiscale Phase Separation. Advanced Materials, 2019, 31, e1806547.	21.0	155
121	Rational Design of TiC-Supported Single-Atom Electrocatalysts for Hydrogen Evolution and Selective Oxygen Reduction Reactions. ACS Energy Letters, 2019, 4, 126-132.	17.4	104
122	Electrocatalysts with Increased Activity for Coelectrolysis of Steam and Carbon Dioxide in Solid Oxide Electrolyzer Cells. ACS Catalysis, 2019, 9, 967-976.	11.2	21
123	Cu-Pd alloy nanoparticles as highly selective catalysts for efficient electrochemical reduction of CO2 to CO. Applied Catalysis B: Environmental, 2019, 246, 82-88.	20.2	167
124	Suppression of Cation Segregation in (La,Sr)CoO <sub>3â^'δ</sub> by Elastic Energy Minimization. ACS Applied Materials & Interfaces, 2018, 10, 8057-8065.	8.0	44
125	2â€{ <i>N</i> â€Methylbenzyl)pyridine: A Potential Liquid Organic Hydrogen Carrier with Fast H <sub>2</sub> Release and Stable Activity in Consecutive Cycles. ChemSusChem, 2018, 11, 641-641.	6.8	1
126	2â€( <i>N</i> â€Methylbenzyl)pyridine: A Potential Liquid Organic Hydrogen Carrier with Fast H <sub>2</sub> Release and Stable Activity in Consecutive Cycles. ChemSusChem, 2018, 11, 661-665.	6.8	60

#	Article	IF	CITATIONS
127	Mechanistic insight into the quantitative synthesis of acetic acid by direct conversion of CH4 and CO2: An experimental and theoretical approach. Applied Catalysis B: Environmental, 2018, 229, 237-248.	20.2	59
128	Density functional theory study for the enhanced sulfur tolerance of Ni catalysts by surface alloying. Applied Surface Science, 2018, 429, 87-94.	6.1	26
129	Enhanced oxygen exchange of perovskite oxide surfaces through strain-driven chemical stabilization. Energy and Environmental Science, 2018, 11, 71-77.	30.8	75
130	Highly Durable Platinum Singleâ€Atom Alloy Catalyst for Electrochemical Reactions. Advanced Energy Materials, 2018, 8, 1701476.	19.5	152
131	Active site structure of a lithium phosphate catalyst for the isomerization of 2,3-epoxybutane to 3-buten-2-ol. Molecular Catalysis, 2018, 445, 133-141.	2.0	0
132	Sr Segregation in Perovskite Oxides: Why It Happens and How It Exists. Joule, 2018, 2, 1476-1499.	24.0	255
133	Atomic and Molecular Adsorption on the Bi(111) Surface: Insights into Catalytic CO <sub>2</sub> Reduction. Journal of Physical Chemistry C, 2018, 122, 23084-23090.	3.1	48
134	Fully Dispersed Rh Ensemble Catalyst To Enhance Low-Temperature Activity. Journal of the American Chemical Society, 2018, 140, 9558-9565.	13.7	170
135	Low-temperature direct synthesis of high quality WS2 thin films by plasma-enhanced atomic layer deposition for energy related applications. Applied Surface Science, 2018, 459, 596-605.	6.1	42
136	Chemisorption of NH <sub>3</sub> on Monomeric Vanadium Oxide Supported on Anatase TiO <sub>2</sub> : A Combined DRIFT and DFT Study. Journal of Physical Chemistry C, 2018, 122, 16674-16682.	3.1	36
137	Self-assembled alloy nanoparticles in a layered double perovskite as a fuel oxidation catalyst for solid oxide fuel cells. Journal of Materials Chemistry A, 2018, 6, 15947-15953.	10.3	77
138	Synergistic Effect of Molecular-Type Electrocatalysts with Ultrahigh Pore Volume Carbon Microspheres for Lithium–Sulfur Batteries. ACS Nano, 2018, 12, 6013-6022.	14.6	100
139	A novel strategy to develop non-noble metal catalyst for CO2 electroreduction: Hybridization of metal-organic polymer. Applied Catalysis B: Environmental, 2018, 236, 154-161.	20.2	43
140	Tuning the electronic state of metal/graphene catalysts for the control of catalytic activity <i>via</i> N- and B-doping into graphene. Chemical Communications, 2018, 54, 7147-7150.	4.1	13
141	A Simple Descriptor to Rapidly Screen CO Oxidation Activity on Rare-Earth Metal-Doped CeO2: From Experiment to First-Principles. ACS Applied Materials & Interfaces, 2017, 9, 15449-15458.	8.0	59
142	Observation of crystalline changes of titanium dioxide during lithium insertion by visible spectrum analysis. Physical Chemistry Chemical Physics, 2017, 19, 13140-13146.	2.8	10
143	Adsorption differences between low coverage enantiomers of alanine on the chiral Cu{421} <sup>R</sup> surface. Physical Chemistry Chemical Physics, 2017, 19, 13562-13570.	2.8	6
144	Role of Halide Ions for Controlling Morphology of Copper Nanocrystals in Aqueous Solution. ChemistrySelect, 2017, 2, 4655-4661.	1.5	16

#	Article	IF	CITATIONS
145	High-performance Fe 5 C 2 @CMK-3 nanocatalyst for selective and high-yield production of gasoline-range hydrocarbons. Journal of Catalysis, 2017, 349, 66-74.	6.2	20
146	Mechanistic study for enhanced CO oxidation activity on (Mn,Fe) co-doped CeO 2 (111). Catalysis Today, 2017, 293-294, 82-88.	4.4	32
147	Facile Twoâ€Step Synthesis of Allâ€Inorganic Perovskite CsPbX <sub>3</sub> (X = Cl, Br, and I) Zeolite‥ Composite Phosphors for Potential Backlight Display Application. Advanced Functional Materials, 2017, 27, 1704371.	14.9	223
148	A platinum catalyst deposited on a zirconia support for the design of lithium–oxygen batteries with enhanced cycling ability. Chemical Communications, 2017, 53, 11767-11770.	4.1	9
149	Enzymeâ€Driven Hasselbackâ€Like DNAâ€Based Inorganic Superstructures. Advanced Functional Materials, 2017, 27, 1704213.	14.9	33
150	Promoting Effects of Hydrothermal Treatment on the Activity and Durability of Pd/CeO <sub>2</sub> Catalysts for CO Oxidation. ACS Catalysis, 2017, 7, 7097-7105.	11.2	151
151	Different catalytic behaviors of Pd and Pt metals in decalin dehydrogenation to naphthalene. Catalysis Science and Technology, 2017, 7, 3728-3735.	4.1	38
152	Aerosol Cross-Linked Crown Ether Diols Melded with Poly(vinyl alcohol) as Specialized Microfibrous Li <sup>+</sup> Adsorbents. ACS Applied Materials & Interfaces, 2017, 9, 42862-42874.	8.0	47
153	Exsolution trends and co-segregation aspects of self-grown catalyst nanoparticles in perovskites. Nature Communications, 2017, 8, 15967.	12.8	305
154	Design of lithium selective crown ethers: Synthesis, extraction and theoretical binding studies. Chemical Engineering Journal, 2017, 326, 921-933.	12.7	78
155	Understanding the Reaction Mechanism of Glycerol Hydrogenolysis over a CuCr <sub>2</sub> O <sub>4</sub> Catalyst. ChemSusChem, 2017, 10, 442-454.	6.8	13
156	Safe and Ecological Refluxing with a Closed‣oop Air Cooling System. ChemSusChem, 2017, 10, 461-465.	6.8	1
157	Sponge-Like Li <sub>4</sub> Ti <sub>5</sub> O <sub>12</sub> Constructed on Graphene for High Li Electroactivities. Journal of Nanoscience and Nanotechnology, 2017, 17, 588-593.	0.9	3
158	Mechanistic study of glycerol dehydration on Brønsted acidic amorphous aluminosilicate. Journal of Catalysis, 2016, 341, 33-43.	6.2	46
159	Exploring crystal phase and morphology in the TiO 2 supporting materials used for visible-light driven plasmonic photocatalyst. Applied Catalysis B: Environmental, 2016, 198, 91-99.	20.2	20
160	Tunable lithium storage properties of metal lithium titanates by stoichiometric modulation. Electrochemistry Communications, 2016, 64, 26-29.	4.7	8
161	Concentration Effect of Reducing Agents on Green Synthesis of Gold Nanoparticles: Size, Morphology, and Growth Mechanism. Nanoscale Research Letters, 2016, 11, 230.	5.7	76
162	Effect of caffeic acid adsorption in controlling the morphology of gold nanoparticles: role of surface coverage and functional groups. Physical Chemistry Chemical Physics, 2016, 18, 27775-27783.	2.8	22

#	Article	IF	CITATIONS
163	Suppressing cation segregation on lanthanum-based perovskite oxides to enhance the stability of solid oxide fuel cell cathodes. RSC Advances, 2016, 6, 69782-69789.	3.6	41
164	Direct access to aggregation-free and small intermetallic nanoparticles in ordered, large-pore mesoporous carbon for an electrocatalyst. RSC Advances, 2016, 6, 88255-88264.	3.6	12
165	Cold welding of gold nanoparticles on mica substrate: Self-adjustment and enhanced diffusion. Scientific Reports, 2016, 6, 32951.	3.3	20
166	Liquid-liquid extraction of lithium using lipophilic dibenzo-14-crown-4 ether carboxylic acid in hydrophobic room temperature ionic liquid. Hydrometallurgy, 2016, 164, 362-371.	4.3	48
167	Insights into the Li Diffusion Dynamics and Nanostructuring of H <sub>2</sub> Ti <sub>12</sub> O <sub>25</sub> To Enhance Its Li Storage Performance. ACS Applied Materials & Interfaces, 2016, 8, 12186-12193.	8.0	8
168	Density Functional Theory Study for Catalytic Activation and Dissociation of CO <sub>2</sub> on Bimetallic Alloy Surfaces. Journal of Physical Chemistry C, 2016, 120, 3438-3447.	3.1	152
169	Defect-engineered graphene chemical sensors with ultrahigh sensitivity. Physical Chemistry Chemical Physics, 2016, 18, 14198-14204.	2.8	110
170	First-Principles Study of Enhanced Oxygen Incorporation Near the Grain Boundary on Yttria-Stabilized Zirconia. Science of Advanced Materials, 2016, 8, 196-200.	0.7	8
171	Investigation of LiO2 Adsorption on LaB1â^'xB′xO3(001) for Li-Air Battery Applications: A Density Functional Theory Study. Journal of the Korean Ceramic Society, 2016, 53, 306-311.	2.3	2
172	Energy and dose dependence of proton-irradiation damage in graphene. RSC Advances, 2015, 5, 31861-31865.	3.6	21
173	Gas-phase dehydration of vicinal diols to epoxides: Dehydrative epoxidation over a Cs/SiO2 catalyst. Journal of Catalysis, 2015, 323, 85-99.	6.2	31
174	Tuning the Surface Chemistry of Chiral Cu(531) <sup><i>S</i></sup> for Enhanced Enantiospecific Adsorption of Amino Acids. Journal of Physical Chemistry C, 2015, 119, 15195-15203.	3.1	16
175	Interfacial Adsorption and Redox Coupling of Li <sub>4</sub> Ti <sub>5</sub> O <sub>12</sub> with Nanographene for High-Rate Lithium Storage. ACS Applied Materials & Interfaces, 2015, 7, 16565-16572.	8.0	32
176	Omnidirectionally stretchable, high performance supercapacitors based on a graphene–carbon-nanotube layered structure. Nano Energy, 2015, 15, 33-42.	16.0	39
177	Radial alignment of c-channel nanorods in 3D porous TiO2 for eliciting enhanced Li storage performance. Chemical Communications, 2015, 51, 15019-15022.	4.1	11
178	Precise control of defects in graphene using oxygen plasma. Journal of Vacuum Science and Technology A: Vacuum, Surfaces and Films, 2015, 33, .	2.1	32
179	Universality in surface mixing rule of adsorption strength for small adsorbates on binary transition metal alloys. Physical Chemistry Chemical Physics, 2015, 17, 3123-3130.	2.8	27
180	Rational Design of a Bifunctional Catalyst for the Oxydehydration of Glycerol: A Combined Theoretical and Experimental Study. ACS Catalysis, 2015, 5, 82-94.	11.2	34

#	Article	IF	CITATIONS
181	Effect of B-Cation Doping on Oxygen Vacancy Formation and Migration in LaBO <sub>3</sub> : A Density Functional Theory Study. Journal of the Korean Ceramic Society, 2015, 52, 331-337.	2.3	9
182	Promoting alkali and alkaline-earth metals on MgO for enhancing CO <sub>2</sub> capture by first-principles calculations. Physical Chemistry Chemical Physics, 2014, 16, 24818-24823.	2.8	37
183	Kinetic and Mechanistic Insights into the All-Solid-State Z-Schematic System. Journal of Physical Chemistry C, 2014, 118, 29583-29590.	3.1	15
184	Scalable Oxygenâ€lon Transport Kinetics in Metalâ€Oxide Films: Impact of Thermally Induced Lattice Compaction in Acceptor Doped Ceria Films. Advanced Functional Materials, 2014, 24, 1562-1574.	14.9	65
185	Investigation of the adsorption of amino acids on Pd(111): A density functional theory study. Applied Surface Science, 2014, 301, 199-207.	6.1	13
186	A Tailored Catalyst for the Sustainable Conversion of Glycerol to Acrolein: Mechanistic Aspect of Sequential Dehydration. ChemSusChem, 2014, 7, 2193-2201.	6.8	25
187	All-solid-state, origami-type foldable supercapacitor chips with integrated series circuit analogues. Energy and Environmental Science, 2014, 7, 1095.	30.8	62
188	Hybrid MnO2 Film with Agarose Gel for Enhancing the Structural Integrity of Thin Film Supercapacitor Electrodes. ACS Applied Materials & Interfaces, 2013, 5, 9908-9912.	8.0	45
189	Cation Size Mismatch and Charge Interactions Drive Dopant Segregation at the Surfaces of Manganite Perovskites. Journal of the American Chemical Society, 2013, 135, 7909-7925.	13.7	468
190	Mechanism for enhanced oxygen reduction kinetics at the (La,Sr)CoO3â^î(/(La,Sr)2CoO4+δ hetero-interface. Energy and Environmental Science, 2012, 5, 8598.	30.8	109
191	Enantiospecific Chemisorption of Amino Acids on Step Decorated Chiral Cu Surfaces. Topics in Catalysis, 2012, 55, 243-259.	2.8	20
192	New Insights into the Strain Coupling to Surface Chemistry, Electronic Structure, and Reactivity of La <sub>0.7</sub> Sr <sub>0.3</sub> MnO <sub>3</sub> . Journal of Physical Chemistry Letters, 2011, 2, 801-807.	4.6	145
193	Surface Electronic Structure Transitions at High Temperature on Perovskite Oxides: The Case of Strained La <sub>0.8</sub> Sr <sub>0.2</sub> CoO <sub>3</sub> Thin Films. Journal of the American Chemical Society, 2011, 133, 17696-17704.	13.7	148
194	Enhanced one dimensional mobility of oxygen on strained LaCoO3(001) surface. Journal of Materials Chemistry, 2011, 21, 18983.	6.7	64
195	Chirality and Rotation of Asymmetric Surface-Bound Thioethers. Journal of Physical Chemistry C, 2011, 115, 897-901.	3.1	29
196	Density Functional Theory Study of H and CO Adsorption on Alkali-Promoted Mo <sub>2</sub> C Surfaces. Journal of Physical Chemistry C, 2011, 115, 6870-6876.	3.1	59
197	Chemical speciation of adsorbed glycine on metal surfaces. Journal of Chemical Physics, 2011, 135, 034703.	3.0	20
198	Strain Effects on the Surface Chemistry of La0.7Sr0.3MnO3. ECS Transactions, 2011, 35, 2097-2104.	0.5	12

#	Article	IF	CITATIONS
199	Enantiospecific adsorption of amino acids on hydroxylated quartz (101̄0). Physical Chemistry Chemical Physics, 2010, 12, 8024.	2.8	31
200	Step decoration of chiral metal surfaces. Journal of Chemical Physics, 2009, 130, 124710.	3.0	27
201	Enantiospecific Adsorption of Amino Acids on Hydroxylated Quartz (0001). Langmuir, 2009, 25, 10737-10745.	3.5	29
202	Importance of Kinetics in Surface Alloying: A Comparison of the Diffusion Pathways of Pd and Ag Atoms on Cu(111). Journal of Physical Chemistry C, 2009, 113, 12863-12869.	3.1	46
203	First principles calculations of methylamine and methanol adsorption on hydroxylated quartz (0001). Surface Science, 2008, 602, 2478-2485.	1.9	25
204	Optimization of Scaffold for a Successful Hydrogel-Seeding Method for Vascular Tissue Engineering. Key Engineering Materials, 2007, 342-343, 333-336.	0.4	3
205	Characterization of the Gel-Spun Tubular Scaffold for Cardiovascular Tissue Engineering. Key Engineering Materials, 2007, 342-343, 321-324.	0.4	0